IEEE Access
Multidisciplinary | Rapid Review | Open Access Journal

Received January 13, 2019, accepted January 25, 2019, date of publication January 31, 2019, date of current version February 14, 2019.

Digital Object Identifier 10.1109/ACCESS.2019.2896345

Effect of Boundary Condition and Model Structure Integrity of Tooth-PDL-Bone Complex on Tooth Mode Computation

YANGZHOU GAN[1], (Member, IEEE), JING XIONG[1], (Member, IEEE), QUNFEI ZHAO[2], AND ZEYANG XIA[1], (Senior Member, IEEE)

[1]Shenzhen Institutes of Advanced Technology, Chinese Academy of Sciences, Shenzhen 518055, China
[2]Department of Automation, Shanghai Jiao Tong University, Shanghai 200240, China

Corresponding author: Zeyang Xia (zy.xia@siat.ac.cn)

This work was supported in part by the National Natural Science Foundation of China under Grant 61601452, in part by the Guangdong Natural Science Funds for Distinguished Young Scholar under Grant 2015A030306020, in part by the Youth Innovation Promotion Association, Chinese Academy of Sciences, under Grant 2015301, and in part by the Shenzhen Research Project under Grant JCYJ20170818162801483, Grant GJHS20160331185913023, and Grant GJHS20170314154158554.

ABSTRACT Tooth mode has been proven to be adaptable for the diagnosis of periodontal disease. However, in previous studies of tooth mode computation, model settings, including boundary condition and model structure integrity, were quite different. Whether these settings themselves would significantly affect computation results were unknown, and consistent settings that provide support for the generalization of results are desired. This paper aimed to study this by investigating the effect of three commonly used boundary conditions and model structure integrity on tooth mode computation. Three finite-element models of the mandibular tooth-periodontal ligament-bone complex (TPBC) with different levels of structure integrity were constructed. For each model, tooth modes under three boundary conditions were computed, respectively, using modal analysis. Six order modes of each tooth were extracted. The same order mode shapes of different teeth were the same. Compared to the difference of natural frequency (NF) between healthy and periodontal disease, the difference of computed NF of a tooth caused by different boundary condition settings was slight, and the difference of computed NF of a tooth caused by model integrity was slight. The results suggest that the effect of the three boundary conditions and structure integrity of the TPBC model on mode computation of a given tooth is neglectable. Therefore, to compute the mode of a given tooth, these settings can be selected regarding other issues instead of differences caused by these settings themselves.

INDEX TERMS Finite element analysis, modal analysis, tooth mode, boundary condition, model structure integrity.

I. INTRODUCTION

The vibration behavior of a tooth reflects the periodontal status including conditions of periodontal damage, periodontal attachment decay, and alveolar bone loss [1]. The natural frequency (NF) is one type of resonance frequency of a vibrating object. Previous studies have shown evidence that the NF of a tooth provides an important reference for the evaluation of the periodontal health status [1]–[6]. Compared to the traditional radiographic evaluation for periodontal health status, the NF analysis does not involve radiation and is more sensitive to periodontal status changes [2]. Thus, it might be more suitable for early diagnosis and long-term observation of periodontal disease which not only affects individual's oral health but also has an association with the development of various systemic diseases including cardiovascular disease, respiratory disease, diabetes, stroke, and so on [7]–[9].

There are two methods to estimate the NF of a tooth: *in vivo* or *in vitro* experimental method and the computational method. *In vivo* or *in vitro* experimental method commonly applies an impulse force to tested tooth

The associate editor coordinating the review of this manuscript and approving it for publication was Bora Onat.

and receives and analyzes the impact signal to evaluate the NF of the tooth [2], [6], [10], [11]. In this method, the estimated NF is recorded as the frequency where peak amplitude of the received signal occurs. It is approximate to the resonant frequency which results from superimposing external forced vibration on NF profile rather than a free vibration. Thus, this kind of method may fail to obtain accurate vibratory characteristics of tooth [5]. The frequency scanning interval of *in vivo* or *in vitro* experiments may also be simply too large to capture all NFs. Additionally, since the NF of a tooth can be affected by several factors, this kind of method is infeasible to analyze the effect of these individual factors on the estimated NF [12]. Computational method normally uses finite element method (FEM) [13]–[15] and has advantages to simulate free vibration of structure, complex geometric shapes, material properties, and different periodontal conditions, which are difficult to replicate in *in vivo* or *in vitro* experiments. The FEM has been extensively applied to analyze the NFs of teeth [1], [2], [4], [5], different periodontal conditions' effect on NFs [1], [3], [16], and NF values of implants for stability evaluation [12], [17]–[22].

In the computational method represented by FEM, the vibration behavior of a given subject is characterized by the subject' modes which consist of NFs and mode shapes. Boundary condition is an important aspect in the mode computation. Based on different hypothesis, there were mainly three kinds of boundary conditions used in previous studies: node fixation on mesial-distal side surface of bone [8], [11], [16], [18]–[21], node fixation on base surface of bone [5], [23], [24], and node fixation on lateral and base surface of bone [7], [12], [17]. Since these boundary conditions mainly change degrees of freedom of bone and do not directly constrain the vibration of teeth, whether these settings significantly affect the computation results of tooth modes and how to choose a proper boundary condition for the mode computation is unknown. In addition, most of these studies used the sectioned models which only contained the target tooth and its surrounding tissue. Although Liao et al.'s [5] work has indicated that the structure integrity of computational model would considerably affect the vibratory behaviors of the whole system, how the structure integrity of computational model would affect the vibratory behaviors of target tooth is still unknown. A common knowledge regarding this issue is needed as consistent model settings are the foundation of result generalization.

Therefore, this study aimed to investigate the effect of different model settings, including boundary condition and model structure integrity, on the computation of tooth modes. Three anatomical accurate finite element models of mandibular tooth-periodontal ligament (PDL)-bone complex (TPBC) [25] with different levels of structure integrities were generated from cone beam computer tomography (CBCT) images. For each model, three boundary conditions were used as controls to analyze their effect on the computation of tooth modes.

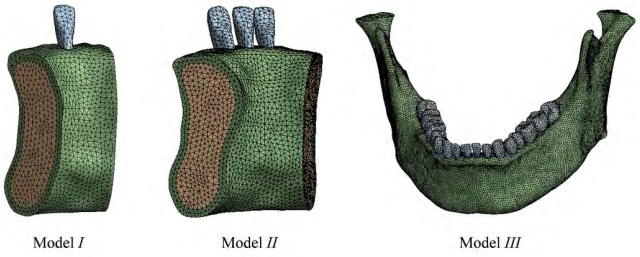

FIGURE 1. The three finite element models of TPBC system used in this study. *Model I*: TPBC model with left central incisor, *Model II*: TPBC model with left lateral incisor, left central incisor, and right central incisor, and *Model III:* TPBC model with full teeth.

II. MATERIALS AND METHODS

A. TPBC MODELING

This study was reviewed and approved by Institutional Review Board of Shenzhen Institutes of Advanced Technology, Chinese Academy of Sciences. Written informed consents of the subjects were obtained. Mandibular TPBC model of one subject (male, 19 years old) with healthy periodontal condition was generated from CBCT images with isotropic spacial resolution of 0.25 mm. To generate the model, two-dimensional (2D) contours of individual teeth and bone were segmented from the CBCT images using threshold and hybrid level set model segmentation method [24], [26] developed in our previous work. The cortical bone and cancellous bone were then separated from the bone region using a local adaptive threshold segmentation method [27]. And the segmentation procedure were implemented using our own code under Matlab platform. Surface models of teeth and bone (including cancellous bone and cortical bone) were reconstructed from the segmented 2D contours using marching cube algorithm [28]. The reconstructed surface models were then imported into Geomagic (Raindrop Geomagic Inc., NC, USA) to generate solid models. The PDLs were obtained through Boolean operation between models of teeth and bone with a uniform thickness of 0.25 mm [15], [29].

To investigate the effect of TPBC structure integrity on tooth mode computation, three mandibular TPBC models with different levels of structure integrities were used. They are: (*I*) TPBC model with left central incisor, (*II*) TPBC model with left lateral incisor, left central incisor, and right central incisor, and (*III*) TPBC model with full teeth, respectively. Model *I* and model *II* were both sectioned from model *III*. The three models were meshed in ANSYS V15.0 (ANSYS Inc., PA, USA) using 10-node tetrahedral element with the same meshing settings as tetrahedral element has better capability to accommodate complicated geometry than hexahedral element [30], [31]. A convergence test [32] was conducted to validate the mesh density of the FE model for discretization approximation. After meshing, there were 60,644 nodes and 36,847 elements for model *I*, 99,938 nodes and 60,403 elements for model *II*, and 812,215 nodes and 499,625 elements for model *III*, respectively. Fig. 1 shows the three FE models used in this study.

TABLE 1. Material property settings of Tooth, Pdl, and Bone.

Tissue	Young's Modulus (MPa)	Poisson' Ratio	Density (kg/m^3)
Tooth	1.66×10^4	0.31	2,200
PDL	0.71	0.40	1,100
Cancellous bone	5.00×10^2	0.38	1,400
Cortical bone	1.00×10^4	0.26	1,400

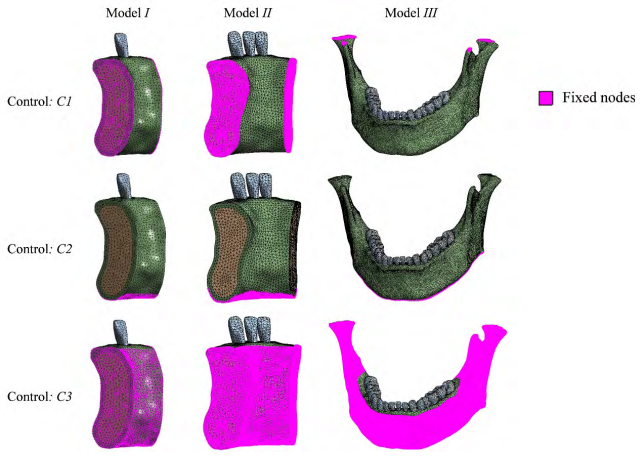

FIGURE 2. Boundary conditions used as controls of each TPBC model. *C1*: node fixation on mesial-distal side surface of bone, *C2*: node fixation on base surface of bone, and *C3*: node fixation on lateral and base surface of bone. For model *III*, *C1* was set to fix nodes on the top surfaces of bone near the temporomandibular joints.

B. MATERIAL PROPERTIES

In this study, all material properties were assigned to be homogeneous, isotropic, and linearly elastic to control the computational complexity as widely used in previous studies [3], [4], [16], [23]. The values of material properties were set based on previous studies [23], [25] (shown in Table 1).

C. BOUNDARY CONDITIONS

Tooth, PDL, cancellous bone, and cortical bone in each FE model were set to be bonded with their neighbors. For each model, three boundary conditions were used as controls to explore their effect on tooth mode computation. The three boundary conditions were: (*C1*) node fixation (in this study the node fixation means that all the six degrees of freedom of node are fixed) on mesial-distal side surface of bone, (*C2*) node fixation on base surface of bone, and (*C3*) node fixation on lateral and base surface of bone (shown in Fig. 2). For model *III*, as there was no sectioned surface on the mesial-distal sides of bone, *C1* was set to fix nodes on the top surfaces near the temporomandibular joints [33].

D. TOOTH MODE COMPUTATION

The modal analysis in ANSYS was used to compute tooth modes. After the computation of modal analysis converged, the value of each order's NF and the corresponding mode

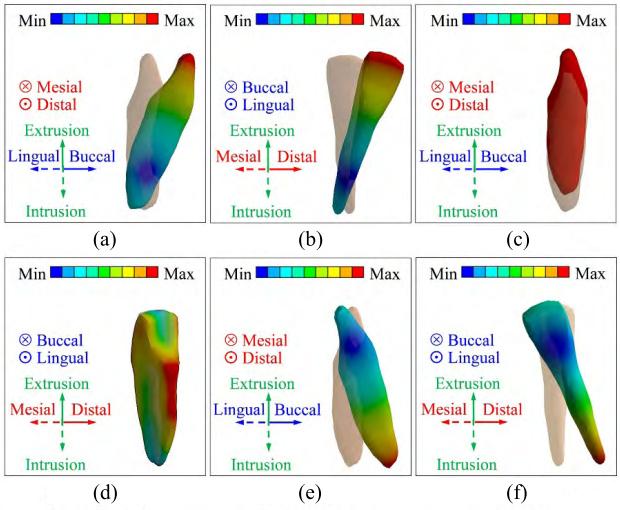

FIGURE 3. The six mode shapes of a left central incisor. The vibrational mode shapes are compared to their original shapes. In the vibrational shapes, different colors from blue to red denote vibrational amplitudes from small to large.

shapes in terms of vibrating pattern can be read directly from the results. The directly obtained modes reflect the vibration properties of the TPBC system, and not all modes are associated with the vibrational behavior of teeth since lots of regions in the system have the potential to vibrate. Additionally, there are multiple order modes for each tooth [1], [4], [5]. To obtain all potential modes of each tooth, under any of the three boundary conditions the first 20, 50, and 200 modes of TPBC system were calculated for the model *I*, model *II*, and model *III*, respectively. Tooth modes were then extracted from associated modes of TPBC system. In a certain mode of TPBC, if any tooth occurred as primary vibrating part and vibration of the local region of bone surrounding the tooth was negligible, this tooth was regarded as a primary vibrating tooth and one mode of this tooth could be extracted. In the nth mode of TPBC, if a tooth occurred as primary vibrating tooth, one mode of the tooth was extracted from the nth mode of TPBC system based on the following definition:

(1) The NF of the tooth was equivalent to that of the TPBC system.

(2) The mode shape of the tooth was determined according to the vibration pattern of the primary vibrating tooth.

(3) The order of this mode was defined to be $m+1$, where m ($m \geq 0$) denoted the number of modes of this tooth which has been extracted from the first $n-1$ modes of TPBC.

III. RESULTS

A. TOOTH MODES OF MODEL I

Using each of the three boundary conditions, six order modes of the left central incisor were extracted from model *I*. The same order modes obtained using different boundary conditions presented the same mode shapes (shown in Fig. 3). The 1st and 2nd mode shapes corresponded to crown swing in buccal-lingual direction and mesial-distal direction, respectively. The 3rd mode shape corresponded to whole

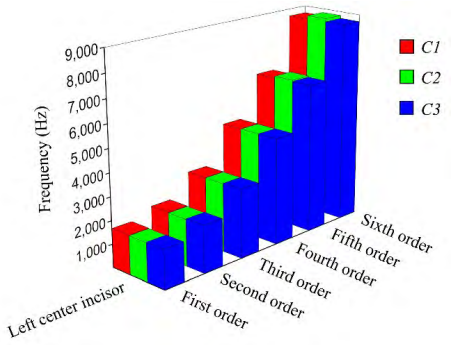

FIGURE 4. Comparison of tooth natural frequencies obtained from model *I* using three different boundary conditions as controls. *C1*: node fixation on mesial-distal side surface of bone. *C2*: node fixation on base surface of bone. *C3*: node fixation on lateral and base surface of bone.

tooth vibration along its axis in extrusion-intrusion direction. The 4th mode shape corresponded to whole tooth twist about its axis. The 5th and 6th mode shapes corresponded to root swing in buccal-lingual direction and mesial-distal direction, respectively.

The corresponding NFs of the left central incisor were presented in Fig. 4 (see Table 2 in Appendix for the value of NFs). The maximum relative difference (i.e. the ratio between the maximum absolute difference of the NFs and the arithmetic mean of the NFs) of the same order NFs obtained using different boundary conditions was 1.66%.

B. TOOTH MODES OF MODEL II

Using each of the three boundary conditions, six order modes of each of the three teeth were extracted from model *II*. For each tooth, the same order mode shapes obtained using different boundary conditions were the same. Additionally, the same order mode shapes of different teeth were the same and in accordance with that extracted from model *I*. The corresponding NFs of the three teeth were presented in Fig. 5 (see Table 3 in Appendix for the value of NFs). Among the three teeth, the maximum relative difference of the same order NFs obtained using different boundary conditions was 2.00%.

C. TOOTH MODES OF MODEL III

In model *III*, there were sixteen teeth. This study focused on the modes of the fourteen teeth from left second molar to right second molar, as the two third molars are generally not the concerns of clinical treatment or lab study. Using each of the three boundary conditions, six order modes of each tooth were extracted from model *III*. For each tooth, the same order mode shapes obtained using different boundary conditions were the same. Additionally, the same order mode shapes of different teeth were the same and in accordance with that extracted from model *I*. The corresponding NFs of the fourteen teeth were presented in Fig. 6 (see Table 4 in Appendix for the value of NFs). Among these teeth, the maximum relative difference of the same order NFs obtained using different boundary conditions was 2.83%.

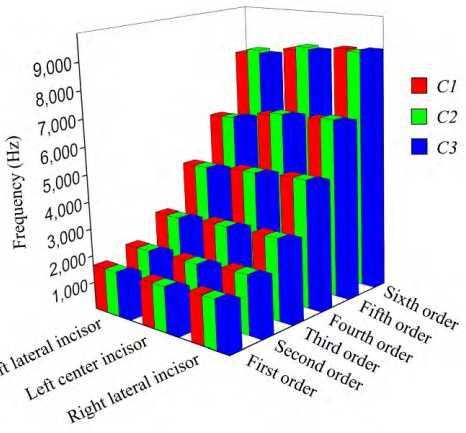

FIGURE 5. Comparison of tooth natural frequencies obtained from model *II* using three different boundary conditions as controls. *C1*: node fixation on mesial-distal side surface of bone. *C2*: node fixation on base surface of bone. *C3*: node fixation on lateral and base surface of bone.

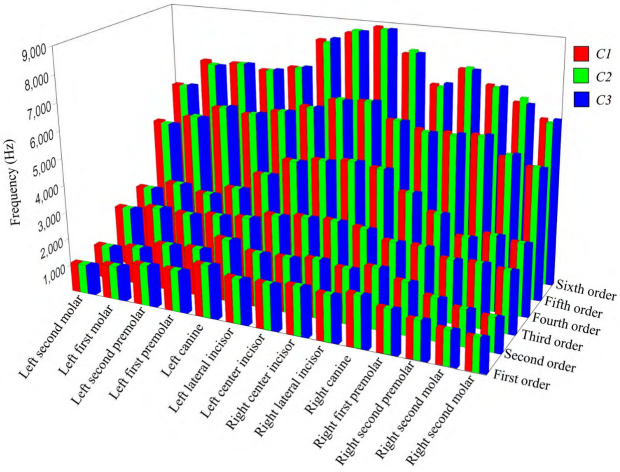

FIGURE 6. Comparison of tooth natural frequencies obtained from model *III* using three different boundary conditions as controls. *C1*: node fixation on top surfaces of bone near the temporomandibular joints. *C2*: node fixation on base surface of bone. *C3*: node fixation on lateral and base surface of bone.

IV. DISCUSSION

A. EFFECT OF DIFFERENT BOUNDARY CONDITIONS ON TOOTH MODE COMPUTATION

The tooth mode computation results showed that the same order mode shapes of a given tooth obtained using the three different boundary conditions were the same, but the same order NFs of a given tooth obtained using the three different boundary conditions were different. In the evaluation of periodontal health status using NFs of target tooth, the first order NF was most widely used. For model *I*, model *II*, and model *III*, the maximum absolute difference of a given tooth's first order NFs computed using the three different boundary conditions were 23.1 Hz, 28.4 Hz, and 25.5 Hz, respectively. And the corresponding maximum relative difference were 1.39%, 1.72%, and 1.31%, respectively. As reported in Huang *et al.*'s [2] work, the difference of the first order NFs of anterior teeth between healthy and periodontal

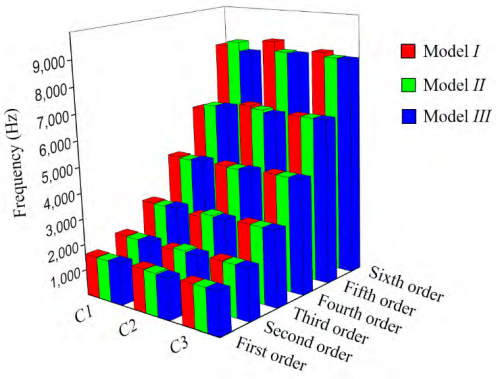

FIGURE 7. Comparison of left central incisor natural frequencies computed from model *I*, model *II*, and model *III* under a given boundary condition. *C1*: node fixation on mesial-distal side surface of bone. *C2*: node fixation on base surface of bone. *C3*: node fixation on lateral and base surface of bone.

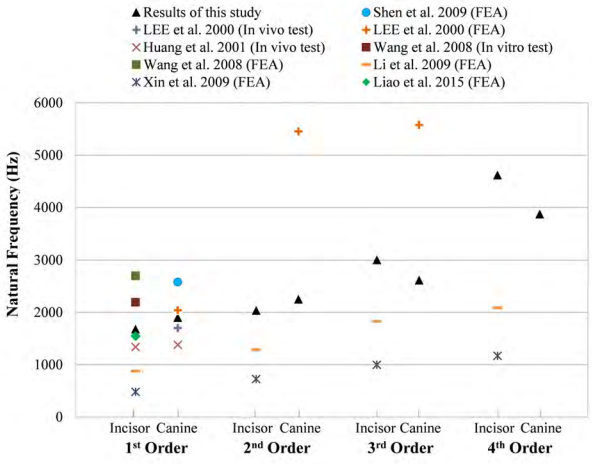

FIGURE 8. Natural frequency comparison of this study to results reported in previous studies.

disease was about 80 Hz, and the corresponding relative difference was about 6.15%. Compared to the difference of NF between healthy and periodontal disease, the effect of the three boundary conditions on NF computation of the tested three models was neglectable. To estimate the mode of a given tooth, the researchers may select the boundary conditions regarding other issues.

However, the three boundary conditions considerably affected the mode computation results of TPBC system. Since nodes of bone were fixed, the primary vibration parts of the same order modes computed using the three different boundary conditions occurred at different position, especially for model *III*. The differences of NFs of the same order modes computed using the three different boundary conditions were also distinct. Taking the first order as example, the maximum relative difference of NFs computed using different boundary conditions were 36.8%, 40.8%, and 67.9% for model *I*, model *II*, and model *III*, respectively. Therefore, to estimate the modes of the whole TPBC system, the selection of boundary conditions is an important consideration.

B. EFFECT OF MODEL STRUCTURE INTEGRITY ON TOOTH MODE COMPUTATION

Liao *et al.*'s [5] study claimed that structure integrity of computational model of a TPBC considerably affected the characterization of vibratory behaviors. However, the conclusion was reached based on the mode results of the whole TPBC system, and how structure integrity would affect the vibratory behaviors of a given tooth was not investigated. In this study, the modes of the left central incisor extracted from the model *I*, model *II*, and model *III* under a given boundary condition were compared. The results presented in Section 3 have shown that, under any a given boundary condition, the six order mode shapes of the left central incisor extracted from the three models were the same. Fig. 7 presents the NF comparison of the left central incisor extracted from the three models under a given boundary condition.

For *C1*, *C2*, and *C3*, the maximum absolute difference of the left central incisor's first order NFs computed from the three different models were 5.7 Hz, 5.3 Hz, and 17.1 Hz, respectively. And the corresponding maximum relative difference were 0.34%, 0.32%, and 1.03%, respectively. As reported in Huang *et al.*'s [2] work, the difference of the first order NFs of incisor between healthy and periodontal disease was about 100 Hz, and the corresponding relative difference was about 7.75%. Compared to the difference of NF between healthy and periodontal disease, the effect of the model structure integrity on NF computation of the tested incisor was neglectable. Therefore, to estimate the mode of a given tooth, it is not necessary to concern the difference caused by structure integrity of TPBC model.

C. RESULT COMPARISON OF TOOTH MODE COMPUTATION WITH PREVIOUS STUDIES

The mode shapes of tooth obtained in this study were the same with these results of previous studies [1], [3]–[5]. In the aspect of NFs, previous studies mainly reported the quantitative results of the incisor and canine. Fig. 8 presents the NF comparison of this study (results from model *III* using boundary condition *C1*) with the results reported in previous studies. For the incisor, the first order NF (1678 Hz) obtained in this study and Liao *et al.*'s results (1546 Hz) fell in the range between Huang *et al.*' in vivo experiment (1340 Hz) and Wang *et al.*'s in vitro experiment (2194 Hz), while the FEA results of other studies (Wang *et al.*, Li *et al.*, and Xin *et al.*) seemed to be more biased to these clinical results. For the canine, the first order NF (1899.6 Hz) obtained in this study was more consistent with the result of Huang *et al.*' in vivo experiment (1380 Hz) and Lee *et al.*'s in vitro experiment (1704 Hz) than other's FEA results (Lee *et al.* and Shen *et al.*). The good agreement between this study and previous clinical data validated the accuracy of the mode computation of this study.

TABLE 2. Tooth natural frequencies obtained from Model I using different boundary conditions (C1: Node fixation on mesial-distal side surface of bone. C2: Node fixation on base surface of bone. C3: Node fixation on lateral and base surface of bone).

Tooth	Order of mode	NFs obtained using C1 (Hz)	NFs obtained using C2 (Hz)	NFs obtained using C3 (Hz)
Left central incisor	1st order	1673.2	1653.3	1676.4
	2nd order	2039.7	2015.6	2040.7
	3rd order	2988.6	2976.9	2992.4
	4th order	4622.8	4616.8	4624.4
	5th order	6433.7	6517.0	6467.7
	6th order	8692.6	8838.1	8711.0

TABLE 3. Tooth natural frequencies obtained from Model II using different boundary conditions (C1: Node fixation on mesial-distal side surface of bone. C2: Node fixation on base surface of bone. C3: Node fixation on lateral and base surface of bone).

Tooth	Order of mode	NFs obtained using C1 (Hz)	NFs obtained using C2 (Hz)	NFs obtained using C3 (Hz)
Left lateral incisor	1st order	1656.9	1638.4	1666.8
	2nd order	2013.6	2002	2017.5
	3rd order	2870.1	2854.3	2876.8
	4th order	4452.3	4449.6	4456.7
	5th order	6054.6	6067.5	6129.5
	6th order	8281.4	8448.7	8337.9
Left central incisor	1st order	1673.2	1670.4	1679.1
	2nd order	2036.6	2030.8	2040.3
	3rd order	2990.9	2978.8	2998.0
	4th order	4618.5	4616.4	4623.4
	5th order	6397.1	6492.5	6478.2
	6th order	8607.8	8750.2	8665.2
Right central incisor	1st order	1799.2	1783.5	1806.0
	2nd order	2174.6	2167.2	2177.5
	3rd order	3022.3	3015.0	3026.8
	4th order	4725.8	4724.2	4729.4
	5th order	6518.8	6580.4	6553.6
	6th order	8818.7	8750.2	8842.9

D. CONTRIBUTION AND LIMITATION

Tooth modes are associated with periodontal damage, periodontal attachment decay, and alveolar bone loss, and have been widely adopted to evaluate the periodontal status. Computational biomechanics is an important method to estimate tooth modes. Boundary condition is a necessary setting in mode computation using computational biomechanics. Three kinds of boundary conditions have been used in previous studies. But whether these settings affect tooth mode computation results significantly and how to choose a proper boundary condition is unknown. This study investigated the effect of the three commonly used boundary conditions on tooth mode computation by applying three TPBC models with different levels of model integrity. The effect of model integrity on tooth mode computation was also analyzed. Different from previous studies which directly used computed mode results of TPBC system to investigate the tooth vibrational behavior, the conclusion of this study was reached explicitly from tooth modes extracted from that of TPBC system. These conclusions would provide important guidance for future studies of tooth mode computation.

TABLE 4. Tooth natural frequencies obtained from Model III using different boundary conditions (C1: Node fixation on mesial-distal side surface of bone. C2: Node fixation on base surface of bone. C3: Node fixation on lateral and base surface of bone).

Tooth	Order of mode	NFs obtained using C1 (Hz)	NFs obtained using C2 (Hz)	NFs obtained using C3 (Hz)
Left second molar	1st order	1081.9	1093	1098.4
	2nd order	1227.9	1224.8	1228.0
	3rd order	2216.9	2202.0	2217.3
	4th order	2532.5	2521.5	2525.4
	5th order	4761.5	4704.7	4695.9
	6th order	5864.1	5829.0	5885.3
Left first molar	1st order	1260.4	1252.3	1271.8
	2nd order	1383.3	1392.6	1397.4
	3rd order	2414.9	2418.9	2436.1
	4th order	2889.5	2881.3	2885.2
	5th order	5075.2	5143.8	5109.1
	6th order	6948.6	6822.6	6799.5
Left second premolar	1st order	1509.4	1500.6	1524.0
	2nd order	1705.6	1713.7	1717.7
	3rd order	2383.6	2360.7	2370.0
	4th order	2672.5	2668.9	2670.5
	5th order	5600.3	5624.1	5679.1
	6th order	6968.2	6972.8	6988.2
Left first premolar	1st order	1537.5	1536.9	1544.0
	2nd order	1778.3	1777.1	1777.1
	3rd order	2516.9	2498.8	2509.2
	4th order	3060.3	3055.7	3058.9
	5th order	5482.6	5517.3	5553.4
	6th order	6817.9	6822.6	6875.5
Left canine	1st order	1935.1	1934.3	1959.8
	2nd order	2334.3	2310.1	2326.3
	3rd order	2592.0	2608.5	2621.3
	4th order	3764.6	3766.9	3774.1
	5th order	5731.8	5751.9	5775.3
	6th order	7045.6	7028.9	7095.9
Left lateral incisor	1st order	1668.7	1645.3	1658.1
	2nd order	2020.3	2008.0	2015.0
	3rd order	2898.1	2861.5	2870.9
	4th order	4447.9	4426.8	4431.4
	5th order	6058.6	6011.4	6059.3
	6th order	8196.0	8113.4	8283.7
Left central incisor	1st order	1678.9	1670.4	1673.8
	2nd order	2034.6	2038.1	2039.9
	3rd order	3003.0	2981.3	2989.7
	4th order	4617.7	4606.6	4608.6
	5th order	6421.2	6465.0	6433.3
	6th order	8550.2	8660.9	8640.6
Right central incisor	1st order	1795.4	1791.9	1798.4
	2nd order	2168.7	2167.4	2172.0
	3rd order	3036.0	3014.1	3019.7
	4th order	4721.5	4725.8	4729.3
	5th order	6497.2	6503.9	6528.3
	6th order	8860.1	8783.1	8806.9
Right lateral incisor	1st order	1705.6	1692.6	1702.4
	2nd order	2028.8	2018.6	2020.8
	3rd order	2943.0	2899.7	2909.8
	4th order	4607.3	4592.4	4599.8
	5th order	5923.3	5929.4	5921.1
	6th order	7979.0	8113.4	8033.6
Right canine	1st order	1899.6	1878.5	1892.9
	2nd order	2249.4	2240.8	2252.3
	3rd order	2614.6	2602.6	2610.4
	4th order	3871.1	3880.1	3885.6
	5th order	5712.7	5633.8	5628.8
	6th order	6948.6	6879.6	7026.4
Right first premolar	1st order	1604.8	1593.5	1607.4
	2nd order	1935.1	1921.9	1928.7
	3rd order	2614.6	2579.8	2596.5
	4th order	3275.7	3264.1	3268.3
	5th order	5712.7	5633.8	5705.1
	6th order	7621.4	7677.2	7620.6

TABLE 4. ***(Continued.)*** **Tooth natural frequencies obtained from Model III using different boundary conditions (C1: Node fixation on mesial-distal side surface of bone. C2: Node fixation on base surface of bone. C3: Node fixation on lateral and base surface of bone).**

Right second premolar	1st order	1397.3	1406.7	1419.3
	2nd order	1571.1	1542.1	1545.1
	3rd order	2315.1	2307.3	2316.2
	4th order	2558.3	2560.6	2562.1
	5th order	5755.2	5718.6	5786.1
	6th order	7138.7	7068.0	7123.9
Right first molar	1st order	1267.3	1256.3	1269.6
	2nd order	1338.7	1334.8	1337.9
	3rd order	2351.9	2341.3	2357.4
	4th order	2799.2	2782.4	2786.4
	5th order	5079.0	5180.6	5218.0
	6th order	6619.2	6785.4	6596.9
Right second molar	1st order	1198.3	1202.2	1216.1
	2nd order	1236.1	1243.7	1251.3
	3rd order	2258.0	2255.1	2274.8
	4th order	2666.8	2664.5	2668.3
	5th order	4850.2	4862.3	4848.8
	6th order	6128.0	6011.4	6146.0

In this study, all material properties were assigned to be homogeneous, isotropic, and linearly elastic for computational simplicity, and damping effects were not considered. Our future work will try to introduce heterogeneous, anisotropic, non-linearly elastic, and damping property of materials for more accurate results.

V. CONCLUSION

The effect of the three boundary conditions and structure integrity of TPBC model on the mode computation of a given tooth is neglectable. Therefore, to compute the mode of a given tooth, these settings can be selected regarding other issues instead of differences caused by these settings themselves.

APPENDIX

See Tables 2–4.

REFERENCES

[1] H. Xin, Y. Li, L. Zhao, and W. Guo, "Nonlinear finite element analysis of the vibration characteristics of the maxillary central incisor related to periodontal attachment," *Med. Biol. Eng. Comput.*, vol. 47, no. 1, pp. 1189–1195, Nov. 2009.

[2] H.-M. Huang, S.-Y. Lee, C.-Y. Yeh, Y.-S. Wang, W.-J. Chang, and C.-T. Lin, "Natural frequency analysis of periodontal conditions in human anterior teeth," *Ann. Biomed. Eng.*, vol. 29., no. 10, pp. 915–920, Oct. 2001.

[3] S.-Y. Lee, H.-M. Huang, C.-Y. Lin, and Y.-H. Shih, "*In vivo* and in vitro natural frequency analysis of periodontal conditions: An innovative method," *J. Periodontol.*, vol. 71, no. 4, pp. 632–640, Apr. 2000.

[4] M. Y. Li *et al.*, "Modal analysis of maxillary central incisor tooth," *Afr. J. Biotechnol.*, vol. 8, no. 19, pp. 5088–5096, Oct. 2009.

[5] Z. Liao, J. Chen, Z. Zhang, W. Li, M. Swain, and Q. Li, "Computational modeling of dynamic behaviors of human teeth," *J. Biomech.*, vol. 48, no. 16, pp. 4214–4220, Dec. 2015.

[6] M. Nishimura *et al.*, "Periodontal tissue activation by vibration: Intermittent stimulation by resonance vibration accelerates experimental tooth movement in rats," *Amer. J. Orthodontics Dentofacial Orthopedics*, vol. 133, no. 4, pp. 572–583, Apr. 2008.

[7] M. P. Cullinan, P. J. Ford, and G. J. Seymour, "Periodontal disease and systemic health: Current status," *Austral. Dental Journa*, vol. 54, no. S1, pp. S62–S69, Sep. 2009.

[8] R. I. Garcia, M. M. Henshaw, and E. A. Krall, "Relationship between periodontal disease and systemic health," *Periodontology*, vol. 25, no. 1, pp. 21–36, Feb. 2001.

[9] G. Hajishengallis, "Periodontitis: From microbial immune subversion to systemic inflammation," *Nature Rev. Immunol.*, vol. 15, no. 1, pp. 30–44, Dec. 2015.

[10] L. Rasmusson, G. Stegersjö, K.-E. Kahnberg, and L. Sennerby, "Implant stability measurements using resonance frequency analysis in the grafted maxilla: A cross-sectional pilot study," *Clin. Implant Dentistry Rel. Res.*, vol. 1, no. 2, pp. 70–74, Oct. 1999.

[11] C.-H. Wang, H.-W. Liu, K.-L. Ou, N.-C. Teng, J.-J. Yu, and H.-M. Huang, "Natural frequency analysis of tooth stability under various simulated types and degrees of alveolar vertical bone loss," *Proc. Inst. Mech. Eng., H, J. Eng. Med.*, vol. 222, no. 6, pp. 983–989, Sep. 2008.

[12] V. Pattijn, C. Van Lierde, G. Van der Perre, I. Naert, and J. V. Sloten, "The resonance frequencies and mode shapes of dental implants: Rigid body behaviour versus bending behaviour. A numerical approach," *J. Biomech.*, vol. 39, no. 5, pp. 939–947, Jan. 2006.

[13] Y. Zhang, W. Song, M. Karimi, C.-H. Chi, and A. Kudreyko, "Fractional autoregressive integrated moving average and finite-element modal: The forecast of tire vibration trend," *IEEE Access*, vol. 6, pp. 40137–40142, 2018.

[14] D.-P. Xu, H.-W. Lu, Y.-W. Jiang, H.-K. Kim, J.-H. Kwon, and S.-M. Hwang, "Analysis of sound pressure level of a balanced armature receiver considering coupling effects," *IEEE Access*, vol. 5, pp. 8930–8939, 2017.

[15] Z. Wang, J. Ma, and L. Zhang, "Finite element thermal model and simulation for a cylindrical Li-ion battery," *IEEE Access*, vol. 5, pp. 15372–15379, 2017.

[16] L.-K. Shen, H.-M. Huang, J.-J. Yu, S.-Y. Lee, C.-M. Lee, and S.-C. Hsieh, "Effects of periodontal bone loss on the natural frequency of the human canine: A three-dimensional finite element analysis," *J. Dental Sci.*, vol. 4, no. 2, pp. 81–86, Jun. 2009.

[17] L. Capek, A. Simunek, R. Slezak, and L. Dzan, "Influence of the orientation of the Osstell transducer during measurement of dental implant stability using resonance frequency analysis: A numerical approach," *Med. Eng. Phys.*, vol. 31, no. 7, pp. 764–769, Sep. 2009.

[18] H.-M. Huang, S.-Y. Lee, C.-Y. Yeh, and C.-T. Lin, "Resonance frequency assessment of dental implant stability with various bone qualities: A numerical approach," *Clin. Oral Implants Res.*, vol. 13, no. 1, pp. 65–74, Feb. 2002.

[19] H.-M. Huang, D.-Z. Liu, Y.-Y. Shiau, C.-Y. Yeh, C.-T. Lin, and S.-Y. Lee, "Natural frequency assessment of stability of root keeper magnetic devices," *Med. Biol. Eng. Comput.*, vol. 42, no. 3, pp. 388–393, May 2004.

[20] K. Wang, D. H. Li, J. F. Guo, B. L. Liu, and S. Q. Shi, "Effects of buccal bi-cortical anchorages on primary stability of dental implants: A numerical approach of natural frequency analysis," *J. Oral Rehabil.*, vol. 36, no. 4, pp. 284–291, Apr. 2009.

[21] E. M. Zanetti *et al.*, "Modal analysis for implant stability assessment: Sensitivity of this methodology for different implant designs," *Dental Mater.*, vol. 34, no. 8, pp. 1235–1245, Aug. 2018.

[22] M. A. Pérez, P. Moreo, J. M. García-Aznar, and M. Doblaré, "Computational simulation of dental implant osseointegration through resonance frequency analysis," *J. Biomech.*, vol. 41, no. 2, pp. 316–325, Oct. 2007.

[23] H.-M. Huang, K.-L. Ou, W.-N. Wang, W.-T. Chiu, C.-T. Lin, and S.-Y. Lee, "Dynamic finite element analysis of the human maxillary incisor under impact loading in various directions," *J. Endodontics*, vol. 31, no. 10, pp. 723–727, Oct. 2005.

[24] Z. Li, Y. Gan, J. Xion, J. Tan, Z. Xia, and Q. Zhao, "Modal analysis of a tooth-PDL-bone complex," in *Proc. 4th IEEE Int. Conf. Inf. Sci. Technol.*, Shenzhen, China, Apr. 2014, pp. 772–775.

[25] Z. Xia and J. Chen, "Biomechanical validation of an artificial tooth–periodontal ligament–bone complex for *in vitro* orthodontic load measurement," *Angle Orthodontist*, vol. 83, no. 3, pp. 410–417, May 2013.

[26] Y. Gan, Z. Xia, J. Xiong, Q. Zhao, Y. Hu, and J. Zhang, "Toward accurate tooth segmentation from computed tomography images using a hybrid level set model," *Med. Phys.*, vol. 42, no. 1, pp. 14–27, Jan. 2015.

[27] S. D. Yanowitz and A. M. Bruckstein, "A new method for image segmentation," *Comput. Vis., Graph., Image Process.*, vol. 46, no. 1, pp. 82–95, 1989.

[28] W. E. Lorensen and H. E. Cline, "Marching cubes: A high resolution 3D surface construction algorithm," *ACM SIGGRAPH Comput. Graph.*, vol. 21, no. 4, pp. 163–169, 1987.

[29] Z. Xia, F. Jiang, and J. Chen, "Estimation of periodontal ligament's equivalent mechanical parameters for finite element modeling," *Amer. J. Orthodontics Dentofacial Orthopedics*, vol. 143, no. 4, pp. 486–491, Apr. 2013.

[30] J. Gao, W. Xu, and Z. Ding, "3D finite element mesh generation of complicated tooth model based on CT slices," *Comput. Methods Programs Biomed.*, vol. 82, no. 2, pp. 97–105, May 2006.
[31] K. T. Huynh, Z. Gao, I. Gibson, and W. F. Lu, "Haptically integrated simulation of a finite element model of thoracolumbar spine combining offline biomechanical response analysis of intervertebral discs," *Comput.-Aided Design*, vol. 42, no. 12, pp. 1151–1166, Dec. 2010.
[32] W. Li, W. V. Swain, Q. Li, and G. P. Steven, "Towards automated 3D finite element modeling of direct fiber reinforced composite dental bridge," *J. Biomed. Mater. Res. B, Appl. Biomater.*, vol. 74, no. 1, pp. 520–528, Jul. 2005.
[33] N. Yoda, Z. Liao, J. Chen, K. Sasaki, M. Swain, and Q. Li, "Role of implant configurations supporting three-unit fixed partial denture on mandibular bone response: Biological-data-based finite element study," *J. Oral Rehabil.*, vol. 43, no. 9, pp. 692–701, Sep. 2006.

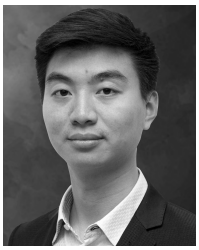

YANGZHOU GAN received the B.S. degree in automation from the University of Electronic Science and Technology of China, in 2010, and the Ph.D. degree in control science and engineering from Shanghai Jiao Tong University, China, in 2015. He is currently an Assistant Professor with the Shenzhen Institutes of Advanced Technology, Chinese Academy of Sciences, Shenzhen, China. His research interests include image processing and biomechanics.

JING XIONG received the B.S. and Ph.D. degrees in mechanical engineering from Tsinghua University, China, in 2004 and 2010, respectively. She is currently an Associate Professor with the Shenzhen Institutes of Advanced Technology, Chinese Academy of Sciences, Shenzhen, China. Her research interests include intelligent robots, medical robots, and imaging guiding key treatment technology.

QUNFEI ZHAO received the B.S.E.E. degree from Xi'an Jiaotong University, China, in 1982, and the Sc.D. degree in system science from the Tokyo Institute of Technology, Japan, in 1988. He is currently a Professor with the School of Electronic Information and Electric Engineering, Shanghai Jiao Tong University, China. His research interests include robotics, machine vision, and optimal control of complex mechatronic systems.

ZEYANG XIA received the B.S. degree in mechanical engineering from Shanghai Jiao Tong University, Shanghai, China, in 2002, and the Ph.D. degree in mechanical engineering from Tsinghua University, Beijing, China, in 2008. He is currently a Professor with the Shenzhen Institutes of Advanced Technology, Chinese Academy of Sciences, Shenzhen, China, and also the Director of the Medical Robotics and Biomechanics Laboratory (http://www.bigsmilelab.ac.cn). He has published over 80 peer-reviewed papers and has applied over 40 patents. His research interests include biped humanoid robotics, medical robotics, and dental biomechanics. He is the Chairman of the Guangzhou Branch of the Youth Innovation Promotion Association, Chinese Academy of Sciences, and the Co-Chair of the Guangdong Chapter of the IEEE Robotics and Automation Society. He served as the Program Co-Chair of the IEEE RCAR 2016 and the ICVS 2017, and will be the General Chair of the IEEE RCAR 2019.